

## RADIO EMISSION FROM SUPERNOVA REMNANTS IN A CLOUDY INTERSTELLAR MEDIUM

R. D. BLANDFORD

W. K. Kellogg Radiation Laboratory, California Institute of Technology

AND

L. L. COWIE

Center for Space Research and Center for Theoretical Physics, Department of Physics, Massachusetts Institute of Technology

Received 1982 January 7; accepted 1982 March 31

### ABSTRACT

We have modified the van der Laan theory of radio emission from supernova remnants to take account of the inhomogeneity of the interstellar medium and to allow for particle acceleration in shock fronts. It is proposed that most of the radio emission in remnants of radius 10–20 pc originates from cold interstellar clouds that have been crushed by the high pressure hot gas within the expanding remnant. It is shown that under these circumstances, simple reacceleration of ambient interstellar cosmic ray electrons can account for the surface brightness-diameter distribution of observed remnants with the additional relativistic particle energy compensating for the decreased filling factor of the radio emitting regions. The model makes interesting predictions about optical and gamma-ray fluxes from the supernova remnants.

Warm ( $\sim 8000$  K) interstellar gas may also be compressed within very large remnants of radius 30–100 pc. This may account for both the giant radio loops when these remnants are seen individually and the anomalously bright galactic nonthermal radio background which may be the superposition of a number of such features. This can provide a reconciliation between the spectrum and intensity of the synchrotron background and the properties of the local cosmic ray electrons. The loops may also produce most of the galactic gamma-ray background.

*Subject headings:* gamma rays: general — interstellar: matter — nebulae: supernova remnants — radio sources: general

### I. INTRODUCTION

Radio emission from supernova remnants of radius  $20 \gtrsim R \gtrsim 10$  pc is usually interpreted in terms of the compression of interstellar cosmic ray electrons and magnetic field behind a cooling shockfront (van der Laan 1962). In general, radio and optical observations of old remnants reveal a shell structure and a correlation between the positions of prominent emission-line and radio features, and this provides impressive support for the general model (e.g., Duin and van der Laan 1975). It has mostly been assumed that the ambient interstellar medium is homogeneous with a typical hydrogen density of order  $1-5 \text{ cm}^{-3}$  and that the shock velocity is roughly  $100 \text{ km s}^{-1}$ , comparable with the observed random motion of the emission-line regions. The structure of the optical and radio emissions is then associated with instabilities in the cooling gas (McCray, Stein, and Kafatos 1975; Duin and van der Laan 1975).

However, supernova remnants in this radius range are known to be X-ray sources (e.g., Gorenstein and Tucker 1976; Tuohy, Nousek, and Garmire 1979) and to emit coronal lines (e.g., Woodgate *et al.* 1974). The associated

temperatures lie in the range  $10^6-10^7$  K, far too high to be associated with a cooling shock wave. This is, however, consistent with the description of the interstellar gas as a multicomponent medium (Cox and Smith 1974; Spitzer 1978; McKee and Ostriker 1977; McCray and Snow 1979). Denser regions which are enveloped by the remnant are crossed by relatively slow, cooling shock waves and are responsible for the optical and radio emission; more diffuse gas remains hot and is responsible for the X-ray emission. In this paper, we will modify the van der Laan model to apply it to a cloudy interstellar medium. In the present view, supernova remnants remain in the adiabatic phase (e.g., Woltjer 1972) throughout the period in which they are observed as radio sources.

As a supernova remnant increases in size, its internal pressure rapidly decreases, and the velocity of a shock driven into a cloud of a given density drops correspondingly. Thus, there exists a radius beyond which clouds of a given density entering a remnant will possess radiative cloud shocks. It is the clouds with densities larger than this value which give rise to the radio and optical emission. Since we do not have more than a general

impression of the spectrum of cloud densities in the ISM, it is important to keep very general the treatment of this aspect of the problem. However, since the bulk of matter in the ISM divides in rough terms into two main phases, there will be two main epochs during which radio emission can be substantially enhanced by the compression mechanism: the conventional "old" supernova remnant epoch ( $R \sim 10\text{--}20$  pc), when the dense clouds are crushed; and the radio loop epoch ( $R \sim 30\text{--}100$  pc), during which the diffuse gas can cool. Gas in a hot phase ( $T \sim 10^6$  K) cannot cool until the end of the remnant's evolution ( $R \gtrsim 100$  pc) (McKee and Ostriker 1977; Cowie, McKee, and Ostriker 1981).

In § II of this paper we give a general discussion of cloud compression and apply it to old remnants in § III. This is then extended to cover radio loops and their contribution to the general galactic radio background in § IV. Some brief comments on the youngest supernova remnants ( $R \sim 2\text{--}10$  pc) are made in § V. Our conclusions are collected in § VI.

## II. COMPRESSION OF INTERSTELLAR GAS WITHIN SUPERNOVA REMNANTS

### a) Crushed Clouds

Consider an adiabatically expanding remnant of age  $1000t_3$  yr, radius  $10R_1$  pc, and energy  $10^{51}E_{51}$  ergs. The mean internal pressure  $\bar{p}$  and effective mean internal hydrogen density  $0.1\bar{n}_{-1}$  cm $^{-3}$  can be defined by the relationships

$$\bar{p} = 5.4 \times 10^{-9} E_{51} R_1^{-3} \text{ dyn cm}^{-2}, \quad (1)$$

$$t_3 = 1.5 \bar{n}_{-1}^{0.5} E_{51}^{-0.5} R_1^{2.5}. \quad (2)$$

(Relations [1] and [2] are consistent with the standard Sedov solution values for uniform gas density.) A dense region of initial hydrogen density  $n$  cm $^{-3}$  (henceforth termed a knot) will be heated by a secondary shock wave driven into it by the high pressure hot gas within the expanding remnant (McKee and Cowie 1975; Chevalier 1977). Significant compression will only occur if this shocked gas can cool in a time  $\sim \bar{p}/|d\bar{p}/dt| \sim t$ . To within a factor  $O(1)$  the shock velocity  $100V_7$  km s $^{-1}$  within the knot is given by

$$V_7 = 7.5 E_{51}^{0.5} R_1^{-1.5} n^{-0.5} \quad (3)$$

(McKee and Cowie 1975). The shock is generally strong and gas-dominated, and so the postshock density and temperature  $T$  are roughly  $4n$  cm $^{-3}$  and  $1.3 \times 10^5 V_7^2 k$ , respectively. The shock can be considered radiative if it can cross a cooling column density in a time  $\sim t$ . Using the cooling column density calculated by McKee and Hollenbach (1980) which takes into account preioniza-

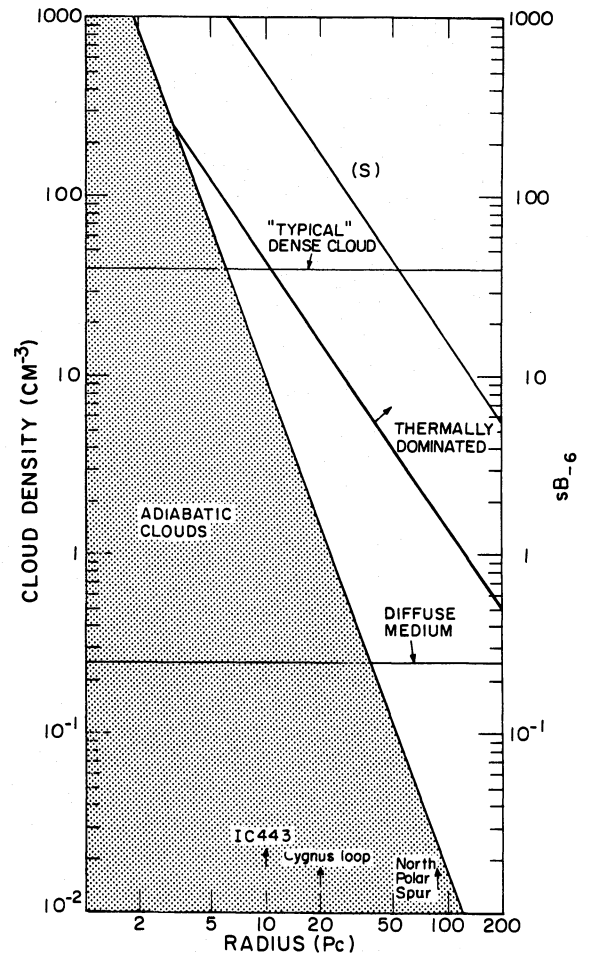


FIG. 1.—The degree of cloud compression as a function of preshock cloud density and remnant radius for a  $10^{51}$  ergs supernova remnant. In the shaded area, the cloud shocks are adiabatic, and there is little compression. The thick solid line (s) with the scale on the right-hand axis shows the compression in a magnetically dominated cloud. Typical positions for phases of the ISM and for various supernova remnants are also indicated.

tion, the condition for a knot to be compressed becomes

$$R_1 > 2.3 E_{51}^{0.29} n^{-0.36} \bar{n}_{-1}^{-0.07}. \quad (4)$$

(Note the insensitivity to  $E$  and  $n$  and especially the most uncertain quantity  $\bar{n}$ .) The corresponding shock velocity is  $\sim 220$  km s $^{-1}$  and is very insensitive to these parameters (cf. Woltjer 1972). Equivalently, clouds of density  $n \gtrsim 10 E_{51}^{0.81} \bar{n}_{-1}^{-0.19} R_1^{-2.8} \equiv n_{\text{cool}}$  will cool. More tenuous clouds will not cool (see Fig. 1).

Clouds that are able to cool will form a thin dense skin of compressed gas. In the absence of extraneous sources of ionization, the gas in this skin will recombine at a temperature  $\sim 5000$  K. If this is the case, then the time an element of gas spends in the recombination zone

$10^3 t_{\text{rec } 3}$  yr is given by

$$t_{\text{rec } 3} \sim 200 s^{-1} n^{-1}, \quad (5)$$

where  $s$  is the total density increase from the unshocked cloud (cf. Shull and McKee 1979).

The ratio of the recombination time to the age  $t$  is typically 0.01–0.3 for the densities that we shall be considering. However, the cloud will evaporate in the hot remnant, and the warm evaporating gas will be a source of ionizing photons. This is hard to quantify, but if the ionizing flux approaches  $\sim 10^8 \text{ cm}^{-2} \text{ s}^{-1}$ , which it probably will do (cf. McKee, Cowie, and Ostriker 1978), then the shell will be maintained in a partially ionized state. Cosmic ray protons trapped within the compressed region provide an additional source of ionization (see below).

The structure of a cooling shock wave is influenced by whether or not preionization can occur. If  $V_7 \geq 1$ , then the preshock gas is ionized. If  $0.7 \leq V_7 \leq 1$ , then the postshock gas is eventually ionized. If  $V_7 \leq 0.7$ , the ionization fraction is always fairly low. As we shall discuss shortly, this influences the relativistic electron acceleration.

Another quantity of interest is the fraction  $\theta$  of the knot crossed by the shock in the remnant age  $t$ , if  $d$  (measured in parsecs) is the smallest dimension of the unshocked knot, then

$$\theta = \min [1, 1.1(\bar{n}_{-1}/n)^{1/2}(R_1/d)]. \quad (6)$$

#### b) Magnetic Field

If, as we shall assume, there is an embedded magnetic field of strength  $B_{-6}$  microgauss in the unshocked gas, then the compression behind the shock will be limited by magnetic pressure. The gas will cool to a temperature in the range 5000–10,000 K and (provided that the ratio of the gas pressure to the magnetic pressure,  $\beta \sim 0.9n \cdot 0.5B_{-6}^{-1}V_7^{-1}$  is less than unity; cf. Fig. 1), the compression ratio in the dense skin on the cloud surface will be

$$s \approx 500 E_{51}^{0.5} B_{-6}^{-1} R_1^{-1.5}. \quad (7)$$

(We have assumed that the magnetic field is randomly directed ahead of the shock so that its strength is increased to a value  $B' \sim (2/3)^{1/2} sB$  within the skin.) In fact, there will be further compression of the gas associated with motion parallel to field. This will occur on a time scale  $\sim 10^5 d$  yr. For the densest clouds within a remnant, the compression may be limited by thermal pressure rather than magnetic when

$$s = 3400 \frac{E_{51} R_1^{-3}}{n}. \quad (8)$$

The actual compression is the minimum of equations (7) and (8).

#### c) Particle Acceleration

We shall generally make a conservative assumption about the degree of particle acceleration. Following Bell (1978*a, b*) and Blandford and Ostriker (1978) we assume that ambient interstellar cosmic ray electrons permeate the knot and are accelerated by the first-order Fermi process at the shock front by scattering off Alfvén waves. We are primarily concerned with relativistic electrons of energy  $\sim 1$  GeV. The locally observed galactic electron spectrum at this energy is uncertain to a factor  $\sim 2$  on account of solar modulation. We adopt a value of  $N_\gamma = 1.7 \times 10^{-15} \text{ cm}^{-3}$  at 1 GeV ( $\gamma = 1960$ ) consistent with a low energy extrapolation of the more accurately determined 10 GeV intensity of Prince (1979) and the most recent study of Webber, Simpson, and Cane (1980). At lower energy, the electron spectrum is conventionally determined from the radio spectrum, which has a spectral index  $\sim 0.6$ , in the direction of the galactic pole (Webber, Simpson, and Cane 1980) consistent with an electron distribution function  $N_\gamma = K\gamma^{-2.2}$ . However, for self-consistency (cf. § IV below), we will adopt a slightly steeper ambient spectrum  $N_\gamma = K\gamma^{-2.4}$  extending down to  $\gamma_{\text{min}} \approx 50$  at which point ionization losses within the Galaxy should flatten the spectrum. Normalizing at 1 GeV gives  $K = 1.3 \times 10^{-7} \text{ cm}^{-3}$ .

As the shock fronts in the clouds are strong with Mach numbers larger than 7, and Alfvén Mach numbers larger than 10, the spectrum of the electrons transmitted by the shock will have a logarithmic slope  $\approx 2.0$  and for  $\gamma \gg \gamma_{\text{min}}$

$$N_\gamma \approx 10K\gamma_{\text{min}}^{-0.4}\gamma^{-2} \approx 3.1 \times 10^{-7}\gamma^{-2} \text{ cm}^{-3}. \quad (9)$$

Efficient acceleration by the Fermi mechanism requires that the Alfvén waves be able to grow faster than ion-neutral collisions can damp them. Both rates are highly uncertain, but using quasi-linear theory for ion-driven Alfvén wave growth (cf. Bell 1978*a*; Blandford and Ostriker 1978), we can estimate the growth and decay rates for the Alfvén waves resonant with 1 GeV cosmic rays

$$\begin{aligned} \Gamma_+ &\sim 10^{-9} V_7 n^{-0.5} \\ \Gamma_- &\sim 3 \times 10^{-11} n \end{aligned} \quad (10)$$

(e.g., Cesarsky 1980). In order to accelerate 1 GeV electrons efficiently, we require that  $n \leq 10V_7^{0.67}$ , a condition that in general is marginally satisfied. By contrast if we adopt the measured cosmic ray mean free paths ( $l \sim 2 \times 10^{12} \text{ cm}$ ) in the interplanetary medium where the values of  $n$ ,  $B$ , and  $v$  are rather similar to those that we expect in an interstellar cloud (e.g., Fisk 1979), then the

associated growth rate is  $\Gamma_+ \sim 2 \times 10^{-9} V_7^2$  which is typically a factor  $\gtrsim 10$  larger than the quasi-linear estimate. The associated time scales ( $\lesssim 100$  yr) and length scales ( $\lesssim 0.01$  pc) are small compared with  $t$  and  $d$ , respectively, and so the acceleration can be regarded as stationary and localized to the neighborhood of the shock front. Note that although the gas cooling length behind the shock is only  $\sim 10^{15}$  cm, the magnetic field will be compressed parallel to the shock front, and postshock diffusion away from the shock front will be strongly inhibited. Reflection by magnetic mirrors will also become important (cf. Morfill, Völk, and Forman 1981).

In deriving these estimates, we have assumed that the preshock gas is ionized. This need not be so if  $V_7 \lesssim 1$ . However, even when the preshock gas is mostly neutral and relativistic electrons can cross the cloud, efficient acceleration can ensue, provided that the shock completely encloses unshocked gas. This is because scattering ahead of the shock affects neither the particle flux at a given energy nor the particle energy gain on crossing the shockfront, and it is precisely these two factors on which the transmitted relativistic electron spectrum depends. Relativistic particles will be reflected by the postshock flow on different sides of the cloud, but the net effect will be the same as if the unshocked interior of the cloud were strongly scattering (Blandford 1982).

There will be further heating of the relativistic electrons associated with the compression that accompanies the radiative cooling. Provided that the relativistic electron pitch angles can be continuously isotropized, then  $N_\gamma$  at a given energy will be increased by a further factor  $(s/4)^{4/3}$ , so that

$$K' \equiv N_\gamma \gamma^2 = 4.3 \times 10^{-8} s^{1.33} \text{ cm}^{-3}. \quad (11)$$

If the electron spectrum in the compressed area extends from  $\gamma_{\min} \sim 50$  to  $\gamma_{\max} \sim 10^4$  (and our results depend only logarithmically upon these choices), then the electron energy density in the compressed gas is a fraction  $\sim 0.12 E_{51}^{-0.33} B_{-6}^{-1.3} R_1$  of the magnetic pressure. The total relativistic electron energy within the compressed regions of the remnant is

$$E_e = 2 \times 10^{47} E_{51}^{0.17} B_{-6}^{-0.33} R_1^{2.5} f \text{ ergs}, \quad (12)$$

where  $f$  was the preshock filling factor of the regions. Cosmic ray protons should likewise be reaccelerated by the shock wave and the subsequent compression. The proton energy density within the compressed area again depends somewhat sensitively upon the ambient interstellar spectrum at sub-GeV energies which is unknown. An estimate, good to a factor of 2, gives a proton energy density in the skin of 10 times the electron energy density, and so if  $R_1 \gtrsim 2 E_{51}^{0.33} B_{-6}^{1.3}$ , the compression may be limited by relativistic proton pressure rather than thermal or magnetic pressure. Furthermore, protons of

energy  $\lesssim 10$  MeV will lose their energy by Coulomb collisions and provide a further source of ionization and consequently of trapping of the relativistic particles.

These estimates probably represent the minimum amount of particle acceleration expected. Particles may also be injected at the shock front and accelerated up to relativistic energies. However, in the case of old supernova remnant shocks with  $V_7 \sim 1$ , this appears to be rather difficult for both electrons and protons (Bell 1978*b*). As an example, consider a preionizing shock with  $V_7 \sim 1$  in a cloud with  $n \sim 1$  and preshock Alfvén speed  $a \sim 3 \text{ km s}^{-1}$ . Mildly suprathermal electrons injected behind the shock with speeds  $\sim 10^4 \text{ km s}^{-1}$  have to cross the shock  $\sim 100$  times to double their energy. Their Larmor radius is  $\sim 10^8 \text{ cm}$ , which is smaller than the expected shock thickness (of order the ion Larmor radius  $\sim 10^9 \text{ cm}$ ). Electrostatic fields in the vicinity of the shock front must be far more important than the first-order Fermi process in accelerating suprathermal electrons. Suprathermal protons with speeds  $\sim 2 \times 10^7 \text{ cm s}^{-1}$  have larger Larmor radii than suprathermal electrons and only have to cross the shock a few times to double their energy. However, as they are moving slowly, they will be subject to strong Coulomb losses in the ionized gas ahead of the shock (e.g., Spitzer 1977). In order that the acceleration time of a suprathermal ion be shorter than the Coulomb loss time ( $\sim 2 \times 10^3 \text{ s}$ ), the scattering mean free path ahead of the shock must be  $\lesssim 10^{10} \text{ cm}$  or about 30 Larmor radii. This in turn implies an amplitude for resonant Alfvén waves ( $\delta B/B$ )  $\gtrsim 0.2$ , many orders of magnitude larger than that expected on the basis of quasi-linear theory. If, by contrast, the cosmic ray pressure behind the shock is of order half the preshock momentum flux as suggested by Eichler (1979), then postshock compression will not occur at all. We shall return to these points in the discussion.

If the gas in the dense skin is able to recombine, then the emitting electrons will probably stream freely away soon after recombination. However, if a high level of ionization can be maintained, as discussed above, then the streaming velocity should be limited to the Alfvén speed. (See Cesarsky 1980 for a discussion of the status of this hypothesis.) The electrons will move along the magnetic field which is aligned parallel to the cloud surface. Under these assumptions the escape time exceeds the expansion time  $t$  for

$$d \gtrsim 0.05 \bar{n}^{-1.5} E_{51}^{-0.25} R_1^{1.75} B_{-6}^{0.5} n^{-0.5}. \quad (13)$$

Likewise, a simple estimate of the ambipolar diffusion time (e.g., Spitzer 1978) gives a time scale  $\sim 10^8 d^2 \alpha n^2 B_{-6}^{-2} s^{-2} \text{ yr}$  for the field to separate from the neutral gas, where  $\alpha$  is the ionization fraction. This is generally larger than the expansion time scale  $t$ , and so we shall henceforth assume that the crushed clouds can



synchrotron radiate for a time  $\sim t$ . However, we should bear in mind that if MHD instabilities allow the particles to escape, then we will have overestimated the surface brightness.

#### d) Synchrotron Emission

We can now compute the synchrotron emission expected from the crushed clouds. The volume emissivity at a frequency  $\nu$ , GHz is  $\epsilon_\nu \sim 1.1 \times 10^{-32} K' B_{-6}^{1.5} \nu_9^{-0.5}$  ergs  $s^{-1} cm^{-3} Hz^{-1}$ . The total luminosity from knots having a preshock density  $n$  is  $L_\nu \sim 4/3 \pi R^3 \epsilon_\nu f(n)/s$ , where  $f(n)$  is the filling factor for clouds of this density. The mean surface brightness across the remnant is  $L_\nu/4\pi^2 R^2$  or evaluating at 408 MHz,

$$\Sigma_{408} = 1.5 \times 10^{-16} E_{51}^{0.9} B_{-6}^{-0.3} f \theta R_1^{-1.8} \text{ ergs cm}^{-2} \text{ s}^{-1} \text{ Hz}^{-1}. \quad (14)$$

Here we have assumed that all of the relativistic electrons within the knots are trapped.

As is well known, synchrotron losses and self-absorption are unimportant at the frequencies of interest. However, free-free absorption within the high density, compressed regions provides an important constraint on models of observed supernova remnants. If we assume unit covering factor, the spectrum should be of the form  $\Sigma_\nu \propto \nu^{-0.5} (1 - e^{-\tau_{ff}})/\tau_{ff}$ , where  $\tau_{ff} \propto \nu^{-2}$  is the free-free optical depth across the remnant. The spectral turnover occurs at an optical depth  $\tau_{ff} \approx 0.5$  or equivalently a frequency

$$\nu_{ff} \approx 70 n f^{0.5} E_{51}^{0.25} R_1^{-0.25} B_{-6}^{-0.5} \text{ MHz}, \quad (15)$$

assuming that the temperature is  $\sim 8000$  K.

A further constraint is provided by the Razin effect when the cloud is ionized. Suppression of the synchrotron emission will occur below a frequency of  $20 n B_{-6}^{-1/2}$  MHz.

### III. RADIO EMISSION FROM $10 < R < 20$ pc SUPERNOVA REMNANTS

#### a) General Remarks

For the older known supernova remnants ( $10 < R < 20$  pc) we are concerned with the dense cold clouds that are believed to contain most of the mass of the interstellar medium ( $n \sim 5-100 \text{ cm}^{-3}$ ). It is clear from the discussion in § II that the compression mechanism is effective over this range of radii. For  $E_{51} \sim 1$  (e.g., Chevalier 1977) and cloud densities in the range  $5 \lesssim n \lesssim 100 \text{ cm}^{-3}$ , cloud crushing will commence at radii  $R_{\min}$  in the range 4–13 pc (see Fig. 1). Preionization and possible fresh electron injection will cease at  $\sim 1.7 R_{\min}$ . For a McKee-Ostriker (1977) “standard cloud”  $n = 40 \text{ cm}^{-3}$ ,

then  $R_{\min} = 6$  pc. For a “diffuse” cloud  $n = 5 \text{ cm}^{-3}$ ,  $R_{\min} = 13$  pc—such relatively diffuse clouds must be invoked to account for the emission from the larger remnants.<sup>1</sup> Before presenting a more detailed discussion, there are a number of important points about the interstellar compression stage of radio remnants which we wish to summarize.

1. The models cannot produce a high enough radio surface brightness to account for remnants younger than  $R \sim 10$  pc, and these must be accounted for by a distinct model (§ V). On morphological grounds (radio polarization, etc.), it is well known that there is a distinction between these two classes of remnants, which reinforces this theoretical consideration.

2. There is likely to be a very large variation in radio surface brightness from remnant to remnant, reflecting variation in the local filling factor of clouds and the cloud density. The model is sensitive to such variations.

3. In particular, we note the possibility that the observed remnants lie at the upper end of the range of  $\Sigma$  at a given remnant radius and that there could exist a class of “radio-quiet” supernova remnants. The known radio SNR would then constitute the class of remnants in which there existed a substantial filling factor of relatively diffuse clouds.

#### b) Surface Brightness

Fermi acceleration at the shock front automatically reproduces the spectral index  $\alpha \sim -0.5$  observed in the majority of old remnants (Clark and Caswell 1976). Free-free absorption and energy-dependent escape can be invoked to account for slightly flatter and steeper spectra, respectively. It is conventional to display the mean surface brightness as a function of the diameter of the supernova remnants.<sup>2</sup> This is done in Figure 2 for remnants of radius  $> 2$  pc, taking data from Clark and Caswell (1976). As we have discussed above, the surface brightness calculated on the basis of this model depends upon the nature of the clouds and the degree of particle acceleration.

We have shown on Figure 2 three  $\Sigma$ - $D$  relations given by the model for various reasonable cloud parameters:

- (a)  $n = 40 \text{ cm}^{-3}$ ,  $f = 0.02$ ,  $B_{-6} = 5$   
(McKee-Ostriker ISM)
- (b)  $n = 40 \text{ cm}^{-3}$ ,  $f = 0.1$ ,  $B_{-6} = 5$   
(Dense region)

<sup>1</sup>This is also true for optical emission (cf. McKee and Cowie 1975).

<sup>2</sup>The distances and hence the diameters of old remnants are notoriously uncertain, and as we noted in § IIIa, the completeness of the sample is extremely dubious. In view of these points it would be a mistake to overinterpret the  $\Sigma$ - $D$  diagram, and in particular there may be many undetected “radio-quiet” remnants.

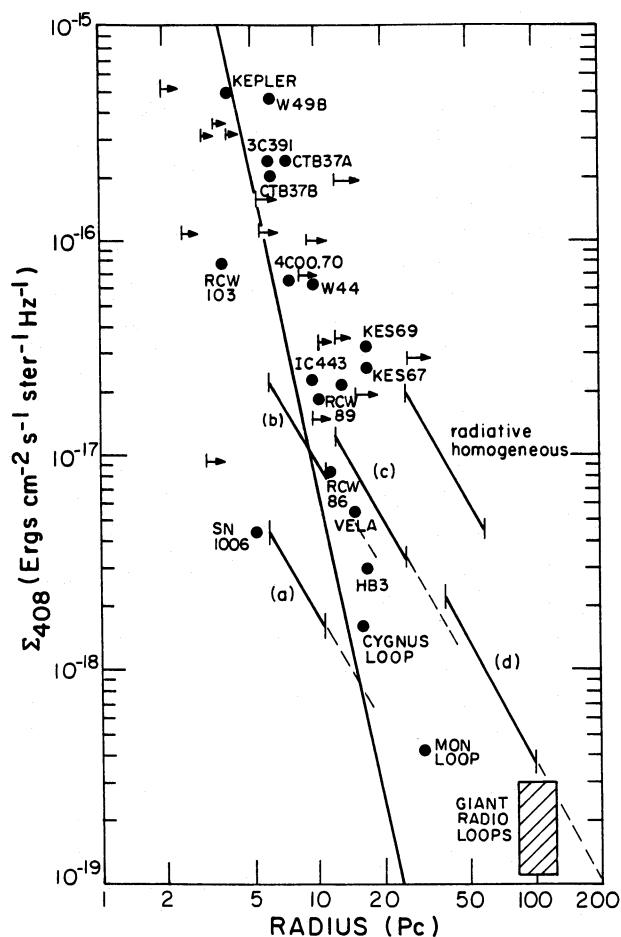


FIG. 2.— $\Sigma$ - $D$  diagram for supernova remnants and giant radio loops. Shown are the primary calibrators of Clark and Caswell 1976 excluding plerions. Where appropriate, distances and diameters have been rescaled to allow for a galactic center-solar distance of 8 kpc. The position of the giant radio loops has been estimated from Berkhuijsen 1972. Also shown are the various models outlined in §§ III b and IV a. The dashed extensions show the region beyond which shock preionization no longer occurs.

$$(c) \quad n = 5 \text{ cm}^{-3}, \quad f = 0.2, \quad B_{-6} = 5$$

(Region of diffuse clouds).

The general ISM may vary considerably and contain both type (a) and type (c) clouds. When this is taken into account the models can account for the observed scatter in  $\Sigma(R)$ .

This model of the radio emission is incompatible with a homogeneous interstellar medium. For example, a homogeneous region with  $n = 1 \text{ cm}^{-3}$  would produce a very bright radio remnant for  $R \geq 20 \text{ pc}$ . The lack of such observed remnants strongly suggests that such regions are very unusual in the interstellar gas into which the remnants evolve.

From equation (15) we see that with our standard models, the free-free absorption turnover should lie in the range  $\sim 70$ – $400 \text{ MHz}$ . The observations have been summarized by Dickel (1973) who states that approximately 5 of 80 sources show substantial curvature at 80 MHz, which in view of the uncertainties is compatible with all of these models. Note the weak dependence on radius. We would expect that remnants with more optical emission should show higher frequency spectral turnovers. Razin suppression should occur at frequency  $\lesssim 160 \text{ MHz}$  (models a, b) and 20 MHz (model c), again compatible with existing spectra.

We have so far assumed that the clouds are small enough to be crossed by the shock in the expansion time ( $\theta = 1$ ) yet large enough to allow the particles to be trapped. Using equation (6) we see that this requires our standard clouds to have smallest dimension  $d \lesssim 0.1 \text{ pc}$ . However from equation (11), we find that clouds this small can be crossed in an Alfvén time. If the model is to be self-consistent, then we must invoke a small degree of disorder in the cloud magnetic fields. In view of the low polarization (see below), this does not seem too unreasonable.

### c) Overall Morphology

The radio emission from unfilled old remnants is generally concentrated in a thick shell and broken up into knots that are generally elongated tangential to the rim of the remnant and are somewhat correlated with the positions of optical emission. There are two explanations for the shell structure in the context of the present model, and both are probably of general importance. First, the interior pressure  $\bar{p}$  is not uniform throughout the remnant. For example in a Sedov solution, the total pressure (ram plus static) increases by a factor of  $\sim 2.5$  from the center to the shock with most of the increase occurring in the outermost 30% of radius. The emissivity per unit volume of unshocked cloud after it has been shocked is roughly proportional to  $p^{-5/4}$ , and so the volume emissivity of the rim should exceed that of the center by at least a factor of  $\sim 3$ . Second, clouds in the interior will be more likely to have been broken up, and this will facilitate escape of the relativistic electrons from the compressed regions.

The elongation of the clouds is to be expected on this model because the largest pressure will be felt on the interior surface of the cloud, and so the shock velocity  $\propto p^{-1/2}$  will be largest here (cf. McKee and Cowie 1975). Also, Duin and van der Laan (1975) proposed that filaments might be produced by thermal instability when the thermal conductivity is small perpendicular to the magnetic field direction.

The surface brightness to be expected from an individual knot can also be calculated. If we retain the assumptions of § II, then the surface brightness of an individual knot exceeds the average surface brightness

by a factor  $\sim (d/t)(d/fR)$ , where  $t$  is the postshock smallest dimension of the knot projected on the plane of the sky. For a typical knot  $d/t$  will be a few, but for edge on knots at the rim, the factor could rise to near the compression factor  $s$  or close to 100 for typical remnants. The most prominent knots should therefore be observed near the rim, where the line of sight passes parallel to the surfaces of the largest crushed clouds. The brightest knots are typically 10 times as bright as the average remnant (e.g., Duin and van der Laan 1975) which requires a filling factor  $f \lesssim 0.1$ . As the filling factor increases (with increasing remnant size) and the radius becomes larger, the contrast of the brightest features should decrease.

#### d) Polarization

The magnetic field changes from being well ordered or predominantly radial in young remnants to being poorly ordered and mainly tangential in old remnants (e.g., Dickel and Milne 1976). As we have discussed, the knots should be flattened into surfaces perpendicular to the remnant radius, and the magnetic field should be preferentially confined to these surfaces. However, acceleration of these crushed clouds and possible magnetic instability will cause a significant radial field component to be produced, which will cause a reduction of the degree of polarization from the maximum expected from synchrotron radiation theory, to the more typically observed value of 10%. We note that the individual bright filaments ought to be polarized parallel to their longest dimensions.

The rotation measures expected from individual knots ( $\approx 100$ – $500$  rad  $m^{-2}$ ) are not incompatible with the values observed (e.g., Dickel and Milne 1976).

#### e) Optical Emission Lines

The radio and optical knots are often correlated in position. It should be possible to quantify this relationship and further constrain the particle acceleration. In particular, by comparing the emissivities for radio and line radiation, we can remove some of the uncertainty concerning the duration of the ionized phase. For example, the ratio of the mean  $H\beta$  and radio surface brightnesses must not be less than the ratio of their volume emissivities in the compressed ionization zone, as there may be evaporation zones which produce lines but not radio synchrotron emission. The total  $H\beta$  luminosity is

$$L_{H\beta} \approx 6 \times 10^{52} \Sigma_{408} B_{-6}^{-0.7} n^2 E_{51}^{-0.4} R_1^{3.3} \text{ ergs s}^{-1}. \quad (16)$$

Unfortunately, this relation is not such a strong constraint because of the fairly powerful dependence upon  $n$ . Model (a) predicts an  $H\beta$  luminosity of  $6 \times 10^{37}$  ergs  $s^{-1}$ ;  $R_1^{1.5}$  and model (b), a luminosity of  $10^{37} R_1^{1.5}$  ergs  $s^{-1}$ . The values are somewhat high and may suggest

that the adopted value of 5 microgauss is too low. More detailed observations of individual filaments are probably necessary to test the relationship underlying equation (16).

An important point to note is that while optical emission-line regions should have associated radio emission (possibly weak), the converse is not true. Clouds which have been fully crossed by the radiative shocks may be hard to detect optically (e.g., McKee *et al.* 1978) while remaining as strongly emitting radio regions.

#### f) Gamma Rays

The relativistic protons and electrons in the crushed clouds will provide a source of  $\gamma$ -rays through  $\pi^0$  decay and electron bremsstrahlung, respectively (Higdon and Lingenfelter 1975; Chevalier 1977). The precise emissivity is somewhat sensitive to the assumed particle spectra on the  $\sim 0.3$ – $1$  GeV energy range, but to sufficient accuracy for present purposes, we can estimate the volume emissivity of  $\gtrsim 100$  MeV  $\gamma$ -rays as

$$\begin{aligned} \epsilon_\gamma \sim & 2 \times 10^{-12} (1 + 0.14\beta) (sn) \\ & \times \left( \frac{p_e}{1 \text{ dyne cm}^{-2}} \right) \text{ cm}^{-3} \text{ s}^{-1}, \quad (17) \end{aligned}$$

where  $p_e$  and  $\beta p_e$  are the cosmic ray electron and proton pressures, respectively. Combining equation (17) with the compression factor calculation of equation (7) and the equation for the total relativistic electron energy (12), we have

$$\dot{N}_\gamma = 6 \times 10^{37} \langle n \rangle E_{51}^{0.67} B_{-6}^{-1.33} R_1 (1 + 0.14\beta) \text{ s}^{-1} \quad (18)$$

for the  $\gamma$ -ray photon production rate of the remnant. Here  $\langle n \rangle \equiv fn$  is the average density of radiatively compressing material entering the remnant.

A typical photon flux obtained from a nearby remnant such as Vela ( $D \approx 500$  pc) obtained by setting  $\langle n \rangle = 1 \text{ cm}^{-3}$ ,  $E_{51} = 1$ ,  $R_1 = 2$ , and  $(1 + 0.14\beta) = 2.4$  is  $9.6 \times 10^{-6} B_{-6}^{-1.33} \text{ cm}^{-2} \text{ s}^{-1}$ . Bennett *et al.* (1977) give an observed upper limit to this quantity of approximately  $10^{-6} \text{ cm}^{-2} \text{ s}^{-1}$  at 100 MeV energies. Correspondingly, the preshock magnetic field in the clouds must exceed 5.5 microgauss. While this conclusion is reasonable, it strongly suggests that the nearby supernova remnants are very close to the present limits of  $\gamma$ -ray detectability.

### IV. RADIO LOOPS AND THE GALACTIC RADIO BACKGROUND

#### a) Warm Interstellar Medium

As we remarked in § I, a significant fraction of the volume of the interstellar medium is in a warm, diffuse phase. This material may also be compressed by a

radiative shock. (It should be noted that for the purposes of the present discussion, it is unimportant whether this component is clumpy as we assumed for the clouds or forms a homogeneous substrate to the denser regions.) For an assumed density  $n \sim 0.3$ , we see from equation (4) with  $E_{51} \sim \bar{n}_{-1} \sim 1$  that cooling will commence at a radius  $R \gtrsim 30$  pc. This component is substantially ionized, and so we do not need the shock to be preionizing for efficient particle acceleration. Postshock compression will again be limited by magnetic pressure, and so we may use equations (12) to estimate the mean surface brightness of the remnant at this radius. For representative values  $f \approx 0.25$  (McKee and Ostriker 1977)  $B_{-6} \approx 3$  (Spitzer 1978) we obtain  $\Sigma_{408} \approx 2.5 \times 10^{-17} R_1^{-1.8}$ . This is shown as line (d) on Figure 2.

### b) Giant Radio Loops

The galactic radio background is not homogeneous but rather contains a variety of radio loops or spurs. It has been widely conjectured that these are fading supernova remnants. In our model, these are naturally identified with the brightest features associated with crushed warm interstellar medium. It is even harder to place these loops on the  $\Sigma$ - $D$  diagram than was the case with the supernova remnants, owing to the large distance uncertainties. Berkhuijsen (1974) gives radii in the range  $\sim 80$ – $120$  pc and corresponding surface brightnesses  $\Sigma_{408} \sim 1$ – $3 \times 10^{-19}$  ergs  $\text{cm}^{-2} \text{s}^{-1} \text{sr}^{-1} \text{Hz}^{-1}$ . These values are entirely compatible with the theoretical estimate of the surface brightness in this phase.

It is very important to emphasize that in a cloudy ISM, the giant radio loops can be formed by supernova remnants of normal energy ( $E_{51} \approx 1$ ) and that indeed such regions are necessarily predicted by the theory.

### c) Gamma-Ray Emission from the Radio Loops

An important corollary to the above discussion is the conclusion that the giant loops should be gamma-ray sources. From equation (18) we obtain

$$\dot{N}_\gamma \approx 2.5 \times 10^{37} R_2 \text{ s}^{-1} \quad (> 100 \text{ MeV}). \quad (19)$$

The gamma-ray surface brightness is then

$$\Sigma_\gamma \approx 7.10^{-6} \text{ cm}^{-2} \text{ s}^{-1} \text{ sr}^{-1}. \quad (20)$$

A loop which would be marginally unresolved by  $\cos B (< 2^\circ)$  would have a flux of  $3 \times 10^{-8} \text{ cm}^{-2} \text{ s}^{-1}$ —about an order of magnitude smaller than is detectable. However, the loops may contribute substantially to the galactic background as we shall discuss in the next subsection.

### d) Contributions to the Galactic Synchrotron and Gamma-Ray Background

The large-scale pressure fluctuations in the galactic pressure induced by the supernova remnants when combined with the cosmic ray acceleration may result in the giant loops being the dominant contribution to the synchrotron and gamma-ray background.

Compression of  $n = 0.3 \text{ cm}^{-3}$  material continues until the pressure within the remnant (eq. [1]) falls below the average ISM value of about  $10^{-12}$  ergs  $\text{cm}^{-3}$ . When radiation is taken into account this occurs at radii of around 100–150 pc (e.g., Cowie, McKee, and Ostriker 1981). For a supernova birthrate of  $S = 10^{-13} S_{-13} \text{ pc}^{-3} \text{ yr}^{-1}$ , the average galactic radio emissivity from the loops is then

$$\langle \epsilon \rangle_{g408} = S \int^{R_{\max}} 4\pi^2 \Sigma(R) R^2 dt, \quad (21)$$

where  $t$  is the age of a loop at radius  $R$ . Setting  $t \sim R^{5/3}$  (McKee and Ostriker 1977),  $R_{\max} = 150$  pc,  $t(R_{\max}) = 7.10^5$  yr (Cowie, McKee, and Ostriker 1981), we obtain

$$\begin{aligned} \langle \epsilon \rangle_{g408} &= 35.2 S \Sigma_{408}(R_{\max}) R_{\max}^2 t_{\max} \\ &= 3.5 \times 10^{-39} S_{-13} \text{ ergs cm}^{-3} \text{ s}^{-1} \text{ Hz}^{-1}. \quad (22) \end{aligned}$$

The uncertainties in  $R_{\max}$ ,  $S_{-13}$  and the preshock magnetic field probably give an uncertainty of about 2 in this value which should be compared with an observed value of about  $7.3 \times 10^{-39}$  ergs  $\text{cm}^{-3} \text{ s}^{-1} \text{ Hz}^{-1}$  (e.g., Webber, Simpson, and Cane 1980).

It has long been known that the galactic radio synchrotron background is roughly 5 times brighter than would be expected on the basis of the locally measured cosmic ray electron intensity and a “standard” interstellar field of order 1–3 microgauss. Another feature is that the slope of the cosmic ray electron spectrum below  $\sim 3$  GeV which is inferred from the radio spectral index appears to be flatter than that measured directly at higher energy. Attempts to account for this often invoke energy-dependent spectral transport within the Galaxy (e.g., Jokipii and Higdon 1978).

We would argue that both features can also be understood using the present model. The particles are freshly reaccelerated within these regions to give a distribution  $N_\gamma \propto \gamma^{-2}$  and a radio spectral index  $\alpha \sim 0.5$  as observed. It is hard to be completely quantitative on the emissivity without a more reliable estimate of the galactic supernova remnant creation rate and the extent of the warm phase, but the estimate given above suggests it is quite likely that most of the radio background be produced in a small fraction of the interstellar volume in overlapping sheets of compressed warm phase interstellar gas.

It is probable that the loops are also responsible for much of the gamma-ray background. The contribution



from the loops to the galactic gamma rays is

$$\dot{N}_{\gamma}(>100 \text{ MeV}) = \frac{1}{\tau} \int_0^{R_{\max}} \dot{N}_{\gamma}(R) dt,$$

where  $\tau$  is the interval between supernovae. Performing the integral and setting  $\tau = 50$  yr,  $R_{\max} = 150$  pc,  $t_{\max} = 7.10^5$  yr:

$$\dot{N}_{\gamma} = 3.10^{41} \text{ photons s}^{-1} \quad (>100 \text{ MeV}).$$

Within the uncertainty in the supernova interval, this could easily account for the entire galactic gamma-ray flux of about  $10^{42}$  photons  $\text{s}^{-1}$  (e.g., Mayer-Hasselwander *et al.* 1981).

#### V. SOME COMMENTS ON YOUNG REMNANTS

The ideas discussed in this paper may have some relevance to young supernova remnants like Cas A ( $R \sim 2$  pc). However, there are a number of difficulties in such an application which would have to be overcome. In these remnants most of the clouds are either gas ejected from the envelope of the exploding star or are lost from the star during its presupernova evolution. These very dense clouds ( $n \sim 1000 \text{ cm}^{-3}$ ) can become radiative within the remnant (Fig. 1; e.g., McKee and Cowie 1975). They may well be identified with the transient knots of high brightness seen in radio maps (Bell 1977). It is not clear what is the appropriate ambient magnetic field within these clouds. However, we know from observation that some knots are so bright that the proton pressure cannot greatly exceed the electron pressure which must have an equipartition value of order one-half the ambient remnant pressure. An additional, selective electron acceleration mechanism must be invoked in young remnants (Bell 1978*b*). Polarization observations give another indication that different processes are at work as magnetic fields in young remnants appear to be more ordered and aligned radially.

#### VI. DISCUSSION

In this paper we have attempted to modify the van der Laan (1962) theory of radio emission from old remnants to take account of the inhomogeneous nature of the interstellar medium. This is made mandatory by soft X-ray and coronal line observations of old remnants. Our theory is based upon an idealized picture of both the interstellar medium and the dynamics of supernova remnants. Observations show quite clearly that on the  $\geq 10$  pc scale, the interstellar medium is nonuniform, and remnants are not circular. Also, both optical and radio studies show that there are long connected filaments extending over a large fraction of the remnant diameter. These are not formed from independent spherical clouds, and a better picture of the dense phase

might be of a loose honeycomb that is readily permeated by the tenuous phase.

Nevertheless, our quantitative conclusions should not be particularly sensitive to these essentially geometrical modifications. What is important is that old remnants have not suffered catastrophic radiative losses and that the filling factor of the denser phases within them is quite small. Our surface brightness estimates are then determined readily by the requirement of pressure equilibrium. In this way we have concluded that clouds will probably be compressed until supported by magnetic stresses, albeit unstably. Fermi reacceleration and compression of ambient galactic cosmic rays can account for the radio surface brightness of the older supernova remnants if we assume that a substantial fraction of the interstellar gas is in the form of relatively diffuse ( $n = 5 \text{ cm}^{-3}$ ) clouds. The optical emission from these remnants suggests a similar result (McKee and Cowie 1975).

We have argued that it is unlikely there is much additional injection of relativistic particles within the radiative cloud shocks. As noted in § II, after compression the clouds are very close to energy equipartition between relativistic protons and magnetic fields. Additional particle acceleration would then decrease the radio surface brightness. Only selective electron acceleration could significantly increase the radio surface brightness (by up to an order of magnitude or so). Ratios of postshock densities inferred from optical line ratios of S II and O II compared to preshock densities inferred from surface brightnesses also suggest substantial compression (McKee and Cowie 1975) and hence only a modest amount of particle injection. It should be noted, however, that direct synchrotron emission from the adiabatically compressed regions is always small even with a substantial amount of particle injection in the faster shocks within the remnant.

In this model the radio observations are coupled directly to optical emission line and  $\gamma$ -ray observations, and this should provide tests of the model. The interpretation of low-frequency radio spectra and polarization measurements is more problematical because these aspects of the observations are quite strongly dependent upon the uncertain geometry.

This model predicts the existence of large radio remnants of radius up to 100 pc and accounts for the gross features of giant radio loops. Giant loops are probably only occasionally distinguished as such, because several remnants can be seen along a line of sight at fairly low galactic latitudes. We have argued that it is the superposition of regions of compressed warm interstellar medium in these large remnants that is responsible for most of the galactic radio synchrotron and gamma-ray backgrounds. This reconciles a number of compatibility problems between the spectrum and surface brightness of the synchrotron background and the local spectrum and intensity of cosmic ray electrons.

We wish to thank A. C. Fabian, C. F. McKee, and J. P. Ostriker for invaluable discussions during the early phases of this work. Helpful comments by A. Achterberg, R. Epstein, and M. McNab are also acknowledged. R. B. acknowledges support under NSF grants AST78-20375 and 80-11752, and the Alfred P.

Sloan Foundation and hospitality at Nordita.

L. L. C. was supported by NASA grants NGL31-001-007 at Princeton and NAGW-208, NSG-7643, and NGL-22-009-638 at MIT and thanks the Fairchild distinguished scholar program at Caltech for support and hospitality during the early portion of this work.

## REFERENCES

- Bell, A. R. 1977, *M.N.R.A.S.*, **179**, 573.  
 ———. 1978a, *M.N.R.A.S.*, **182**, 147.  
 ———. 1978b, *M.N.R.A.S.*, **182**, 443.  
 Bennett K. *et al.* 1977, *Astr. Ap.*, **61**, 279.  
 Berkhuijsen, E. 1974, *Astr. Ap.*, **35**, 429.  
 Blandford, R. D. 1982, in Proceedings NATO Conference on Supernova Remnants, ed. M. J. Rees and R. J. Stoneham, in press.  
 Blandford, R., and Ostriker, J. P. 1978, *Ap. J. (Letters)*, **221**, L29.  
 Cesarsky, C. J. 1980, *Ann. Rev. Astr. Ap.*, **18**, 289.  
 Chevalier, R. A. 1977, *Ap. J.*, **213**, 52.  
 Clark, D. H., and Caswell, J. L. 1976, *M.N.R.A.S.*, **174**, 267.  
 Cowie, L., McKee, C. F., and Ostriker, J. P. 1981, *Ap. J.*, **247**, 908.  
 Cox, D. P. and Smith, B. W. 1974, *Ap. J. (Letters)*, **189**, L105.  
 Dickel, J. R. 1973, *Australian J. Phys.*, **26**, 364.  
 Dickel, J. R., and Milne, D. K. 1976, *Australian J. Phys.*, **25**, 539.  
 Duin, R. M., and van der Laan, H. 1975, *Astr. Ap.*, **40**, 111.  
 Eichler, D. 1979, *Ap. J.*, **229**, 419.  
 Fisk, L. A. 1979, in *Particle Acceleration Mechanisms in Astrophysics*, ed. J. Arons, C. E. Max, and C. F. McKee (New York: American Institute of Physics), p. 63.  
 Gorenstein, P., and Tucker, W. H. 1976, *Ann. Rev. Astr. Ap.*, **14**, 373.  
 Higdon, J. C., and Lingefelter, R. E. 1975, *Ap. J. (Letters)*, **198**, L17.  
 Jokipii, J. R., and Higdon, J. C. 1978, *Ap. J.*, **228**, 293.  
 Mayer-Hasselwander, H. A. *et al.* 1981, *Astr. Ap.*, in press.  
 McCray, R., Stein, R. F., and Kafatos, M. 1975, *Ap. J.*, **196**, 565.  
 McCray, R., and Snow, T. P. 1979, *Ann. Rev. Astr. Ap.*, **17**, 213.  
 McKee, C. F., and Cowie, L. L. 1975, *Ap. J.*, **195**, 715.  
 McKee, C. F., Cowie, L. L., and Ostriker, J. P. 1978, *Ap. J. (Letters)*, **219**, L23.  
 McKee, C. F., and Hollenbach, D. 1980, *Ann. Rev. Astr. Ap.*, **18**, 219.  
 McKee, C. F., and Ostriker, J. P. 1977, *Ap. J.*, **218**, 148.  
 Morfill, G., Völk, H., and Forman, M. 1981, preprint.  
 Prince, T. A. 1979, *Ap. J.*, **227**, 676.  
 Shull, J. M., and McKee, C. F. 1979, *Ap. J.*, **227**, 131.  
 Spitzer, L. 1978, *Physical Processes in the Interstellar Medium* (New York: Wiley Interscience).  
 Tuohy, I., Nousek, J., and Garmire, G. 1979, *Ap. J. (Letters)*, **234**, L101.  
 van der Laan, H. 1962, *M.N.R.A.S.*, **124**, 179.  
 Webber, W. R., Simpson, G. A., and Cane, H. V. 1980, *Ap. J.*, **236**, 448.  
 Woltjer, L. 1972, *Ann. Rev. Astr. Ap.*, **10**, 129.  
 Woodgate, P., *et al.* 1974, *Ap. J. (Letters)*, **188**, L79.

R. D. BLANDFORD: W. K. Kellogg Radiation Laboratory, 106-38, California Institute of Technology, Pasadena, CA 91125

L. L. COWIE: Physics Department, Room 6-209, Massachusetts Institute of Technology, Cambridge, MA 02139